bioRxiv preprint doi: https://doi.org/10.1101/2020.08.03.234708; this version posted August 4, 2020. The copyright holder for this preprint (which was not certified by peer review) is the author/funder, who has granted bioRxiv a license to display the preprint in perpetuity. It is made available under aCC-BY 4.0 International license.

Seed hemicelluloses tailor mucilage properties and salt tolerance

Bo Yang[1,2], Florian Hofmann[1,3], Björn Usadel[1,3,4], Cătălin Voiniciuc [1,2,3]

[1]Institute for Botany and Molecular Genetics (IBMG), BioSC, RWTH Aachen University, 52074 Aachen, Germany; [2]Independent Junior Research Group–Designer Glycans, Leibniz Institute of Plant Biochemistry, 06120 Halle (Saale), Germany; [3]Institute for Bio- and Geosciences (IBG-2: Plant Sciences), Forschungszentrum Jülich, 52425 Jülich, Germany;

[4]Present addresses: Institute for Bio- and Geosciences (IBG-4: Bioinformatics), Forschungszentrum Jülich, 52425 Jülich, Germany; and Institute for Biological Data Science, Heinrich Heine University, 40225 Düsseldorf, Germany;

Author for correspondence:
Cătălin Voiniciuc
Tel: +49 345 5582 1720
Email: catalin.voiniciuc@ipb-halle.de

Key words: germination, glycosyltransferase, hemicellulose, salinity, seed mucilage

E-Mails and ORCiD

B.Y.	bo.yang@ipb-halle.de	0000-0003-4446-0415
F.H.	f.hofmann35@gmail.com	
B.U.	b.usadel@fz-juelich.de	0000-0003-0921-8041
C.V.	catalin.voiniciuc@ipb-halle.de	0000-0001-9105-014X

bioRxiv preprint doi: https://doi.org/10.1101/2020.08.03.234708; this version posted August 4, 2020. The copyright holder for this preprint (which was not certified by peer review) is the author/funder, who has granted bioRxiv a license to display the preprint in perpetuity. It is made available under aCC-BY 4.0 International license.

Summary

- While Arabidopsis seed coat epidermal cells have become an excellent genetic system to study the biosynthesis and structural roles of various cell wall polymers, the physiological function of the secreted mucilaginous polysaccharides remains ambiguous. Seed mucilage is shaped by two distinct classes of highly substituted hemicelluloses along with cellulose and structural proteins, but their interplay has not been explored.
- We deciphered the functions of four distinct classes of cell wall polymers by generating a series of double mutants with defects in heteromannan, xylan, cellulose, or the arabinogalactan protein SALT-OVERLY SENSITIVE 5 (SOS5), and evaluating their impact on mucilage architecture and on seed germination during salt stress.
- We discovered that *muci10* seeds, lacking heteromannan branches, had elevated tolerance to salt stress, while heteromannan elongation mutants exhibited reduced germination in $CaCl_2$. In contrast, xylan made by *MUCILAGE-RELATED21* (*MUCI21*) was found to be required for the adherence of mucilage pectin to microfibrils made by CELLULOSE SYNTHASE5 (CESA5) as well as to a SOS5-mediated network.
- Our results indicate that the substitution of xylan and glucomannan in seeds can fine-tune mucilage adherence and salt tolerance, respectively. The study of germinating seeds can thus provide insights into the synthesis and modification of complex glycans.

Introduction

Cellulose microfibrils are deposited around plant cells and enmeshed in a complex matrix of hemicelluloses, pectin, and, to a lesser extent, structural proteins. The roles of specific classes of cell wall polymers have been difficult to study even in model organisms. For instance, *Arabidopsis thaliana* has nine *CELLULOSE SYNTHASE-LIKE A* (*CSLA*) genes that are at least putatively involved in the synthesis of heteromannan (HM), a class of hemicellulose mainly built of β-1,4-linked mannosyl units. While HM polysaccharides could store carbon to feed growing seedlings or serve as structural cell wall components (Schröder *et al.*, 2009), the physiological roles of these polymers in Arabidopsis are poorly understood because mutation of *CSLA7* is embryo-lethal, but no phenotypic changes were reported in *csla* triple mutant stems lacking detectable HM (Goubet *et al.*, 2009). Significant insights into the biosynthesis and functions of various cell wall components, including HM, have been gained using the Arabidopsis seed coat as a genetic model (Šola *et al.*, 2019). The seed coat epidermis secretes large amounts of

bioRxiv preprint doi: https://doi.org/10.1101/2020.08.03.234708; this version posted August 4, 2020. The copyright holder for this preprint (which was not certified by peer review) is the author/funder, who has granted bioRxiv a license to display the preprint in perpetuity. It is made available under aCC-BY 4.0 International license.

polysaccharides that rapidly swell upon hydration to release non-adherent mucilage as well as an adherent capsule. Unbranched pectin is the dominant mucilage component, but the adherent capsule also contains other polymers typical of secondary cell walls (Voiniciuc *et al.*, 2015c).

In the past decade, several classes of carbohydrate-active enzymes have been found to influence mucilage content and properties (Griffiths & North, 2017; Šola *et al.*, 2019). Pectin adherence to the seed surface is controlled in part by CELLULOSE SYNTHASE 5 (CESA5), a key member of the cellulose synthesis complex (Sullivan *et al.*, 2011; Mendu *et al.*, 2011; Harpaz-Saad *et al.*, 2011; Griffiths *et al.*, 2015). Mucilage adherence also requires the arabinogalactan protein (AGP) SALT-OVERLY SENSITIVE 5 (SOS5), which could be part of a mucilage proteo-glycan or a kinase signalling pathway (Harpaz-Saad *et al.*, 2011; Griffiths *et al.*, 2014). Mucilage synthesis also involves at least two types of hemicellulose branching enzymes. MUCILAGE-RELATED21/MUCILAGE-MODIFIED5 (MUCI21/MUM5) is required for the substitution of xylan (Voiniciuc *et al.*, 2015a) and facilitates pectin-cellulose interactions (Ralet *et al.*, 2016). MANNAN α-GALACTOSYLTRANSFERASE1/MUCILAGE-RELATED10 (MAGT1/MUCI10) functions together with CSLA enzymes to produce galactoglucomannan, a branched HM polymer that influences cellulose deposition and mucilage density (Yu *et al.*, 2014, 2018; Voiniciuc *et al.*, 2015b).

Before the discovery of the minor mucilage components, Arabidopsis seed mucilage was thought to be mainly shaped by pectin content or gelling ability. Biochemical and histological analyses of double mutants have clarified how SOS5 and cellulosic ray-like structures provide two distinct mechanisms to anchor pectin to seeds (Griffiths *et al.*, 2014, 2016; Ben-Tov *et al.*, 2018). However, the functional roles of the highly branched xylan and HM found in mucilage have yet to be evaluated in detail. While seed coats have been involved in embryo protection, seed dormancy, germination and dispersal in angiosperms (Western, 2012; North *et al.*, 2014), the physiological roles of Arabidopsis seed mucilage are still ambiguous. In contrast to the Columbia wild type, varieties with impaired mucilage release (Saez-Aguayo *et al.*, 2014) or adherence (Voiniciuc *et al.*, 2015a) have elevated buoyancy and could be dispersed on water. Seed germination is essential for plant establishment and this early growth stage is when plants are most sensitive to salt stress. Despite this, the impact of Arabidopsis mucilage polymers on salt stress was not previously known.

Materials and Methods

Plant materials

bioRxiv preprint doi: https://doi.org/10.1101/2020.08.03.234708; this version posted August 4, 2020. The copyright holder for this preprint (which was not certified by peer review) is the author/funder, who has granted bioRxiv a license to display the preprint in perpetuity. It is made available under aCC-BY 4.0 International license.

Mutations were genotyped using primers listed in Table S1 and Touch-and-Go PCR (Berendzen *et al.*, 2005). The new double mutants generated in this study have been donated to the Nottingham Arabidopsis Stock Center. Plants were grown in climate-controlled chambers as previously described (Voiniciuc *et al.*, 2015b). The germination assays were performed using seeds produced by plants grown individually in 8 cm round pots at 100-120 µE m^{-2} s^{-1} light, 22 °C and around 60% relative humidity. Seeds from mature, dry plants were harvested, separated from the chaff and stored in separate paper bags (one per plant) in a temperature-controlled laboratory, at 40 to 50% humidity.

Microscopic analyses

Seeds were stained with 0.01% ruthenium red (RR) in 24-well plates and quantified in Fiji (https://fiji.sc/; Schindelin et al., 2012) using established protocols (Voiniciuc *et al.*, 2015b). For staining without shaking, seeds were imbibed in 300 µL of 0.01% RR solution for 15 min. Images were acquired with two stereomicroscope-camera setups: MZ12 with DFC 295, or M165FC with MC170 HD (all from Leica). Mucilage immunolabeling with CCRC-M139 (Carbosource, Complex Carbohydrate Research Center) and counter-staining with S4B (Direct Red 23; Sigma Aldrich) was performed using a published protocol and Leica TCS SP8 confocal setup (Voiniciuc, 2017). Germinated seeds were stained with calcofluor white and propidium iodide (0.05%, w/v, for both dyes) for 10 min, rinsed well with water, and imaged on a Zeiss Imager.Z2 with a 10x Plan-Fluar (NA 0.30), Axiocam 506 , and DAPI/Texas Red filters.

Biochemical analyses

Total mucilage was extracted with a ball mill, hydrolyzed, and quantified via high performance anion exchange chromatography with pulsed amperometric detection (HPAEC-PAD) as previously described (Voiniciuc & Günl, 2016). The quantification of mucilage detachment via HPAEC-PAD has also been described in detail (Voiniciuc, 2016). HPAEC-PAD of mucilage was conducted on a Dionex system equipped with CarboPac PA20 columns (Voiniciuc & Günl, 2016). For alcohol-insoluble residue (AIR) isolation, all material (72 h post-stratification) from four biological replicates was pooled, finely ground and sequentially washed with 70% ethanol, chloroform:methanol (1:1, v/v) and acetone. Monosaccharide content of germinated seed AIR after 2M trifluoroacetic acid hydrolysis was analyzed on a Metrohm 940 Professional IC Vario (Voiniciuc *et al.*, 2019), equipped with Metrosep Carb 2-250/4.0 guard and analytical columns.

Seed germination assay

bioRxiv preprint doi: https://doi.org/10.1101/2020.08.03.234708; this version posted August 4, 2020. The copyright holder for this preprint (which was not certified by peer review) is the author/funder, who has granted bioRxiv a license to display the preprint in perpetuity. It is made available under aCC-BY 4.0 International license.

Around 20 dry seeds (precise number recorded) were incubated in 500 µL of distilled water, 150 mM $CaCl_2$ or 150 mM NaCl in sterile 24-well culture plates (VWR International; 734-2779). Alternatively, seeds were de-mucilaged via ball mill extraction in water (Voiniciuc & Günl, 2016), rinsed well, resuspended in the final solvent and transferred (500 µL) to 24-well plates. All plates had the four corner-wells with only water and were sealed with 3M micropore tape to reduce desiccation. Genotype and replicates were distributed to avoid positional bias. Floating seeds were counted as the number remaining in the center of each well, atop the solution. Plates were stratified for 66 h (dark, 4°C), transferred to a phytochamber (22°C, 100 µE m^{-2} s^{-1} constant light), and then imaged every 24 h with a Leica M165FC stereomicroscope. Seeds were defined as germinated if radicle length was >70 µm, when quantified in Fiji (line tool).

Figures and statistical analysis

Micrographs were processed uniformly in Fiji. Numerical data were plotted as bar graphs in Microsoft Excel 365 or as box/violin plots in the Past 4 statistics software package (https://folk.uio.no/ohammer/past/; Hammer *et al.*, 2001)). Panels were assembled in Inkscape (https://inkscape.org/). ATH1 microarray expression, including GSE20223 dataset (Narsai *et al.*, 2011), was visualized in GENEVESTIGATOR Professional (https://genevestigator.com/). Two-samples and multiple samples statistics were performed in Excel and Past 4, respectively.

Results and Discussion

Mucilage adherence requires multiple wall polymers, except HM

In this study, we dissected the roles of four distinct classes of mucilage polymers by generating a series of double mutants with defects in HM, xylan, cellulose or an AGP (SOS5). We crossed the *muci10-1* (Voiniciuc *et al.*, 2015b) and *muci21-1* (Voiniciuc *et al.*, 2015a) hemicellulose mutants to each other, as well as to *cesa5-1* (Mendu *et al.*, 2011) and *sos5-2* (Harpaz-Saad *et al.*, 2011). The seeds of homozygous single and double mutants had wild-type dimensions but were surrounded by smaller mucilage capsules after shaking and RR staining (Fig. 1). The mucilage capsule area of *muci10* was only 58% of the wild type value and was further reduced in *cesa5, sos5*, *muci21* and respective double mutants. While all mutants produced wild-type percentages of rhamnose and galacturonic acid in total mucilage extracts (Table S2), significant changes in minor sugars were associated with *muci10* (galactose and mannose decreased by >25%) and *muci21* (xylose reduced by >40%) mutations (Fig. 2a). Consistent with previous results (Griffiths *et al.*, 2014), *cesa5* and *sos5* mutations did not alter

bioRxiv preprint doi: https://doi.org/10.1101/2020.08.03.234708; this version posted August 4, 2020. The copyright holder for this preprint (which was not certified by peer review) is the author/funder, who has granted bioRxiv a license to display the preprint in perpetuity. It is made available under aCC-BY 4.0 International license.

matrix polysaccharide composition. The *muci10 muci21* double mutant phenocopied the biochemical deficiencies of the respective single mutants, indicating that xylan and HM substitution can be uncoupled in the seed coat. Sequential mucilage extractions indicated that significantly more pectin (determined as the sum of rhamnose and galacturonic acid) detached from seeds containing *muci21*, *cesa5,* and/or *sos5* mutations compared to wild-type and *muci10* (Fig. 2b and Table S3). Mucilage detachment was also evident when seeds were hydrated directly in RR solution (Fig. 2c). Consistent with 90-92% of pectin detaching from *muci21 cesa5* and *muci21 sos5* seeds, nearly all stained mucilage separated from these seeds even without agitation (Fig. 2b,c). In contrast, the *muci10* mutation only influenced the compactness of pectin, but not its adherence.

Since the *muci10 muci21* double mutant phenocopied the elevated pectin detachment of the *muci21* single mutant (Fig. 2), xylan is likely the main branched hemicellulose responsible for mucilage adherence. Compared to the wild type and *muci10*, unbranched xylan epitopes labelled by the CCRC-M139 monoclonal antibody (Ruprecht *et al.*, 2017) were closer to the surface of *muci21* and *cesa5* seeds, and only diffusely labelled around *sos5* (Fig. S1a). Unlike *muci10*, both *cesa5* and *sos5* mutants increased the detachment of xylose-containing polymers compared to the wild type (Fig. S1b; Table S3). *MUCI21* thus encodes a putative xylosyltransferase, whose activity remains to be confirmed (Voiniciuc *et al.*, 2015a; Zhong *et al.*, 2018), that anchors pectin to the seed coat via potential genetic interactions with *CESA5* and *SOS5*.

When cellulose was stained with S4B (Anderson *et al.*, 2010), *cesa5* and *muci10* mutant seeds showed reduced fluorescence compared to the other single mutants and the wild type (Fig. 2d). In terms of relative cellulose distribution, *muci21* and *sos5* seeds were intermediate to the wild type and the *cesa5* mutant. Consistent with the diffuse xylan immunolabeling (Fig. S1a), *sos5* only displayed diffuse cellulose and lacked ray-like structures (Fig. 2d; Griffiths et al., 2014). Since *muci10* disrupted cellulose architecture more than *cesa5* alone, xylan and SOS5 must be able to anchor *muci10* mucilage to the seed surface despite the loss of cellulosic rays. All double mutants lacked the S4B-stained cellulosic rays found in the wild type (Fig. 2d), so the genetic disruption of any two classes of polymers results in severe mucilage defects.

The elongation and substitution of HM modulate salt tolerance

To investigate the physiological consequences of altered mucilage polysaccharide structure, we established a novel seed germination assay using aqueous solutions in 24-well plates. Nearly all

bioRxiv preprint doi: https://doi.org/10.1101/2020.08.03.234708; this version posted August 4, 2020. The copyright holder for this preprint (which was not certified by peer review) is the author/funder, who has granted bioRxiv a license to display the preprint in perpetuity. It is made available under aCC-BY 4.0 International license.

wild-type and mutant seeds imbibed in water germinated within 24 h post-stratification (Fig. 3a). However, when placed in 150 mM $CaCl_2$, only 12% of wild-type seeds germinated even after 48 h of exposure to constant light. We initially hypothesized that mucilage-defective mutants might be more susceptible to salt stress, but unexpectedly found that *muci10* and *muci10 muci21* seeds had over 5-fold higher germination rate at this stage (Fig. 3a), and displayed longer radicles at 72 h post-stratification (Fig. 3b). The other mutants germinated like the wild type at all time points. Most mutants had around a two-fold higher flotation rate compared to the wild type after a total of five days in 150 mM $CaCl_2$ (Fig. 3c). However, only the radicles of *muci10* and *muci10 muci21* seeds were around 1.7-fold longer than the wild-type after 72 h (Fig. 3d), indicating an unbranched HM-specific effect.

To investigate if the observed tolerance was limited to Ca^{2+} cations, which can cross-link unesterified pectin (Voiniciuc *et al.*, 2015c; Šola *et al.*, 2019), we also treated xylan and mannan mutants with 150 mM NaCl. Compared to water control, both salts reduced the rate of seed germination and inhibited seedling growth (Fig. S2). Although radicles protruded from some NaCl-treated seeds (Fig. S3a), they failed to further elongate compared to the $CaCl_2$ treatment (Fig. S2). All seeds sunk in water within the stratification period (Fig. S4b), but a significant proportion of certain seed varieties continued to float when treated with NaCl (only *muci21*, Fig. S3c), or $CaCl_2$ (most mutants in Fig. 3c). Despite these distinct effects of NaCl and $CaCl_2$, *muci10* and *muci10 muci21* germinated faster than wild type in both salt treatments (Fig. 3a and Fig. S3a).

To elucidate if mucilage alone conferred salt tolerance, we extracted seed coat polysaccharides using a ball mill and repeated the germination assays (Fig. 4). Mucilage removal did not alter the germination rates of after-ripened seeds (Fig. 4a), but significantly reduced the radicle length of each genotype compared to the intact mucilage controls (Fig. 4d). With or without mucilage, $CaCl_2$-treated *muci10* seeds germinated faster and had longer radicles than wild-type seeds. Calcofluor staining at 72 h post-stratification showed that only wild-type seeds, not subjected to mucilage extraction, were surrounded by a capsule containing β-glucans (Fig. 4c). To evaluate the roles of different enzymes involved in HM biosynthesis, we then compared the germination rates of *muci10* and *csla2-3* (Fig. S4), which have similar mucilage defects (Voiniciuc *et al.*, 2015b). $CaCl_2$-treated *csla2* resembled the wild type, but the mannose content of *csla2* germinated seeds was reduced by only 7% (t-test, $P < 0.05$) in either water or $CaCl_2$ (Fig. S4c and Table S4), suggesting that additional CSLAs elongate HM in the same tissues. Using microarray data, we found that the transcription of *CSLA2*, *CSLA3*, *CSLA9* along with *CSLA7* and *CSLA11* (to a lesser extent) increased during germination compared to dry seeds (Fig. S4d). Compared to the wild type, we found that the *csla2-1 csla3-2 csla9-1* triple mutant (hereafter

bioRxiv preprint doi: https://doi.org/10.1101/2020.08.03.234708; this version posted August 4, 2020. The copyright holder for this preprint (which was not certified by peer review) is the author/funder, who has granted bioRxiv a license to display the preprint in perpetuity. It is made available under aCC-BY 4.0 International license.

labelled as *csla239*), reported to have glucomannan-deficient stems (Goubet *et al.*, 2009), had significantly lower germination (Fig. 4b) and smaller radicles (Fig. 4e) in the $CaCl_2$ treatment. The *csla239* triple mutant reduced the mannan content of germinated seeds by one-third (Fig. 3c and Table S5), indicating that even a partial reduction of HM elongation significantly impaired growth under salt stress. Since a *csla7* mutant was defective in embryogenesis (Goubet *et al.*, 2003, 2009), we expect that the full disruption of HM elongation in seeds would be lethal.

In summary, we found that the biosynthesis of two substituted hemicelluloses in the seed coat epidermis can be uncoupled and that HM and xylan have largely independent functions, despite residing in overlapping mucilage regions (Fig. 4f). HM substituted by MUCI10 is mainly responsible for controlling pectin density, supporting cellulose synthesis and modulates seed tolerance to salt stress. In contrast, highly branched xylan made by *MUCI21* is required for the adherence of mucilage pectin to the cellulosic surface of the seed coat, together with *CESA5* and *SOS5*. Branched xylan is required for the adherence of pectin, more than for cellulose, AGPs and HM (Fig. S1 and Table S3). The native localization of the SOS5 AGP protein during seed coat development remains to be confirmed (Fig. 4f) and has been challenging to elucidate (Griffiths *et al.*, 2016). Since *sos5* single mutants did not significantly reduce the content of pectin or cellulose despite altering mucilage staining (Harpaz-Saad *et al.*, 2011; Griffiths *et al.*, 2014), SOS5 primarily influences the distribution of the cellulose-matrix polysaccharide network. In contrast to the role of SOS5 in the apoplast, disruption of cortical microtubule organization inside the seed coat epidermal cells impaired the distribution of cellulose but not mucilage adherence (Yang *et al.*, 2019).

The buoyancy of seeds increases when Ca^{2+} ions cross-link mucilage pectin and the generated double mutants had elevated flotation compared to the wild type. However, only the *muci10* mutation promoted germination under salt stress, while the *csla239* triple mutant reduced it. Consistent with these effects, *MUCI10* and other HM biosynthetic genes were up-regulated during seed germination (Fig. 4g and Fig. S4d), while *MUCI21* was not. Since *CESA5* was also expressed in germinating seeds (Fig. 4g) and *sos5* roots are overly sensitive to salt (no ATH1 microarray probe; Basu *et al.*, 2016), *muci10 cesa5* and *muci10 sos5* double mutants may offset the benefit of *muci10* (Fig. 3). We therefore propose that salt tolerance is enhanced by the presence of unbranched HM, which is more accessible to β-1,4-mannanases (MAN) than its substituted forms. Four *MAN* genes are expressed during Arabidopsis seed imbibition (Fig. 4g), and mutations in *MAN5*, *MAN7*, and particularly *MAN6* reduced germination in favorable conditions (Iglesias-Fernández *et al.*, 2011). MAN enzymes cleave HM polymers, or might potentially remodel the cell wall via transglycosylation activities (Schröder *et al.*, 2009). HM-

bioRxiv preprint doi: https://doi.org/10.1101/2020.08.03.234708; this version posted August 4, 2020. The copyright holder for this preprint (which was not certified by peer review) is the author/funder, who has granted bioRxiv a license to display the preprint in perpetuity. It is made available under aCC-BY 4.0 International license.

derived carbohydrates could provide energy during seed germination or, alternatively, a molecular signal that could enhance salt tolerance. Since only water-treated seedlings accumulated large amounts of glucose (Tables S4 and S5), likely derived from starch, seeds germinating in salt stress might indeed need to mobilize carbon reserves from HM, and to some extent mucilage (Fig. 4), to sustain growth. HM structure, which varies extensively in natural Arabidopsis natural populations (Voiniciuc *et al.*, 2016), therefore represents a novel target to modulate how seeds disperse, germinate and tolerate brackish waters or saline soils containing hostile levels of Ca^{2+} and/or Na^{+}. Consistent with this hypothesis, the constitutive expression of an enzyme involved in producing GDP-mannose, the sugar donor for HM elongation, elevated the mannose content of Arabidopsis seedlings and their tolerance to 150 mM NaCl (He *et al.*, 2017).

In conclusion, we have deciphered the contrasting roles of two classes of hemicelluloses in establishing seed mucilage properties and uncovered new roles for HM elongation and substitution in germination and radicle elongation under salt stress. Since we found that many genes encoding carbohydrate-active enzymes are up-regulated during germination (Fig. 4g and S4d), and multiwell plates are suitable for both microscopic and biochemical analyses of polysaccharides, this cultivation system could speed up our understanding of cell wall biosynthesis and modification. The overlapping expression profile of *MUCI10* with multiple HM-related genes in germinating seeds (Fig. S4d) highlights the need to investigate the specificity of these players on the cellular level in future studies. Further *in vitro* (Liepman *et al.*, 2005; Yu *et al.*, 2018) or synthetic biology (Voiniciuc *et al.*, 2019) approaches are required to elucidate the glycan structures yielded by different HM-related enzymes isoforms, or combinations thereof.

Accession Numbers

MUCI10 (At2g22900); MUCI21 (At3g10320); CESA5 (At5g09870); SOS5 (At3g46550); CSLA2 (At5g22740); CSLA3 (At1g23480); CSLA9 (At5g03760)

Acknowledgements

We thank Stefanie Müller, Benita Schmitz and Stefanie Clauß for excellent technical assistance with plant cultivation. We also grateful to Dr. Debora Gasperini and the Imaging Unit at the Leibniz Institute of Plant Biochemistry for microscope access. The *csla239* triple mutant was kindly provided by Professor Paul Dupree (University of Cambridge). The research was funded in part by the Natural Sciences and Engineering Research Council of Canada (NSERC PGS-D3 to C.V.), Deutsche Forschungsgemeinschaft (DFG research grant 414353267 to C.V.; and

bioRxiv preprint doi: https://doi.org/10.1101/2020.08.03.234708; this version posted August 4, 2020. The copyright holder for this preprint (which was not certified by peer review) is the author/funder, who has granted bioRxiv a license to display the preprint in perpetuity. It is made available under aCC-BY 4.0 International license.

US98/13-1 to B.U.) and by the Ministry of Innovation, Science and Research of North-Rhine Westphalia within the framework of the NRW Strategieprojekt BioSC (No. 313/323-400-00213 to B.U.). Generation of the CCRC series of monoclonal antibodies used in this work was supported by a grant from the NSF Plant Genome Program (DBI-0421683).

Author Contributions:

B.U. and C.V. designed the research. B.U. and C.V. supervised the first and second halves of the project, respectively. B.Y., F.H. and C.V. performed experiments and data analysis. C.V. wrote the article using drafts from B.Y. and valuable feedback from B.U.

Figures

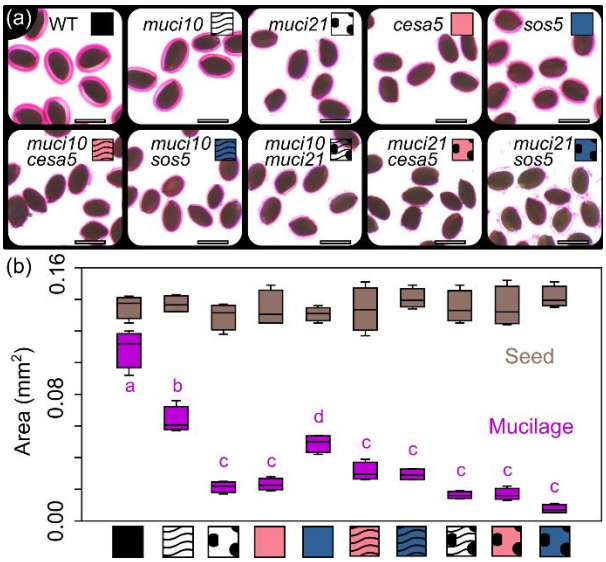

Fig. 1. Dimensions of adherent mucilage capsules. (a) Wild-type (WT) and mutant seeds were gently mixed in water and stained with RR. Scale bars = 0.6 mm. (b) Box plots of projected seed and mucilage areas of four biological replicates (each with an average of 17 quantified seeds) per genotype, labelled according to the legends in (a). Letters denote significant differences (one-way ANOVA with Tukey test, $P < 0.01$).

bioRxiv preprint doi: https://doi.org/10.1101/2020.08.03.234708; this version posted August 4, 2020. The copyright holder for this preprint (which was not certified by peer review) is the author/funder, who has granted bioRxiv a license to display the preprint in perpetuity. It is made available under aCC-BY 4.0 International license.

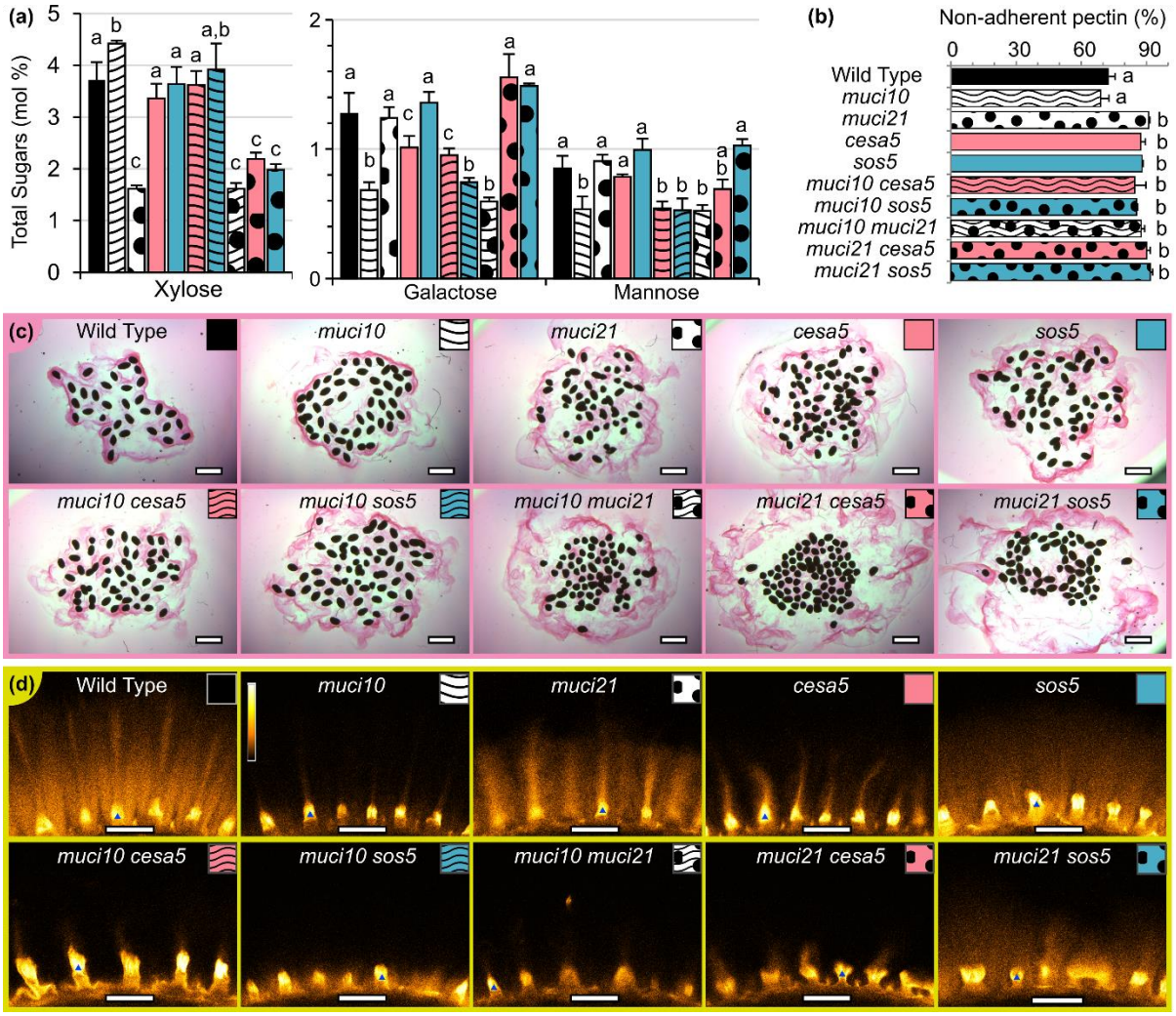

Fig. 2. Mucilage polysaccharide composition and distribution. (a) Content of hemicellulose-derived monosaccharides in total mucilage. (b) The non-adherent proportion of pectin (sum of rhamnose and galacturonic acid). Data show mean + SD of four biological replicates, except only two for sos5 in (b), and letters denote significant differences (one-way ANOVA with Tukey test, $P < 0.05$). (c) Hydration of seeds in RR solution, without shaking. (d) S4B-stained cellulose, coloured using Orange Hot LUT in Fiji (see bar in *muci10* subpanel). Blue triangles mark the seed surface. Scale bars = 1 mm (c), 50 µm (d).

bioRxiv preprint doi: https://doi.org/10.1101/2020.08.03.234708; this version posted August 4, 2020. The copyright holder for this preprint (which was not certified by peer review) is the author/funder, who has granted bioRxiv a license to display the preprint in perpetuity. It is made available under aCC-BY 4.0 International license.

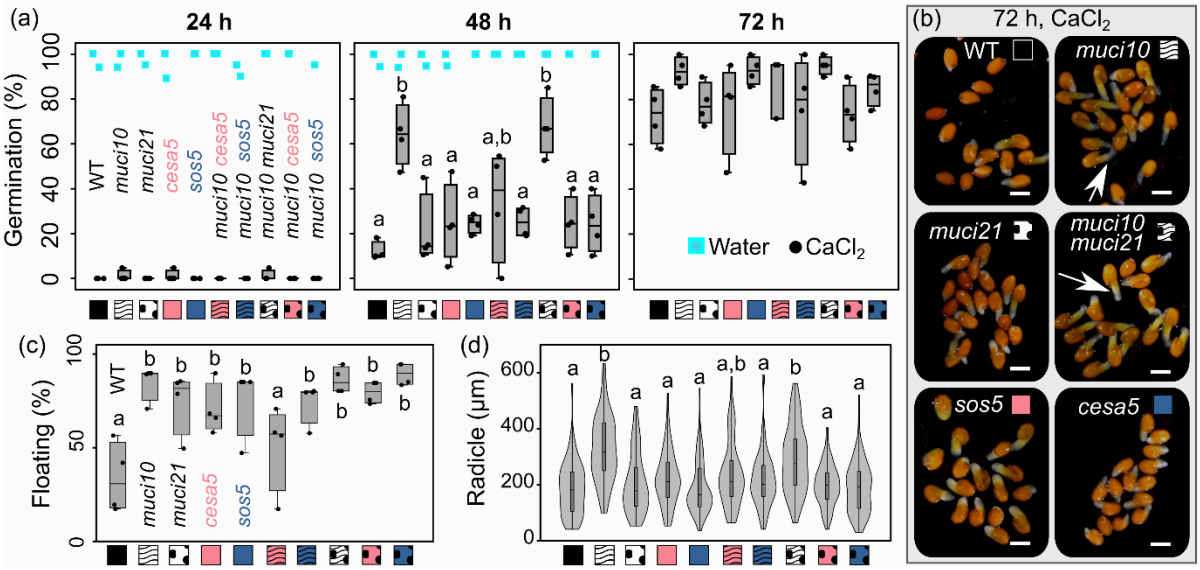

Fig. 3. Germination of seeds in water and $CaCl_2$. (a) Germination of stratified seeds. Box plots show four biological replicates treated with 150 mM $CaCl_2$. In water, nearly all seeds germinated within 24 h. (b) Representative images of germinating seeds; arrows indicate elongated radicles. Scale bars = 500 µm. (c) Box plots of seed flotation. (d) Violin and box plots of the radicle lengths of germinated seeds. Data in (b) to (d) are from the $CaCl_2$ treatment at 72 h. All plots are labeled using the legend in (a), and letters mark significant changes (one-way ANOVA with Tukey test, $P < 0.05$).

bioRxiv preprint doi: https://doi.org/10.1101/2020.08.03.234708; this version posted August 4, 2020. The copyright holder for this preprint (which was not certified by peer review) is the author/funder, who has granted bioRxiv a license to display the preprint in perpetuity. It is made available under aCC-BY 4.0 International license.

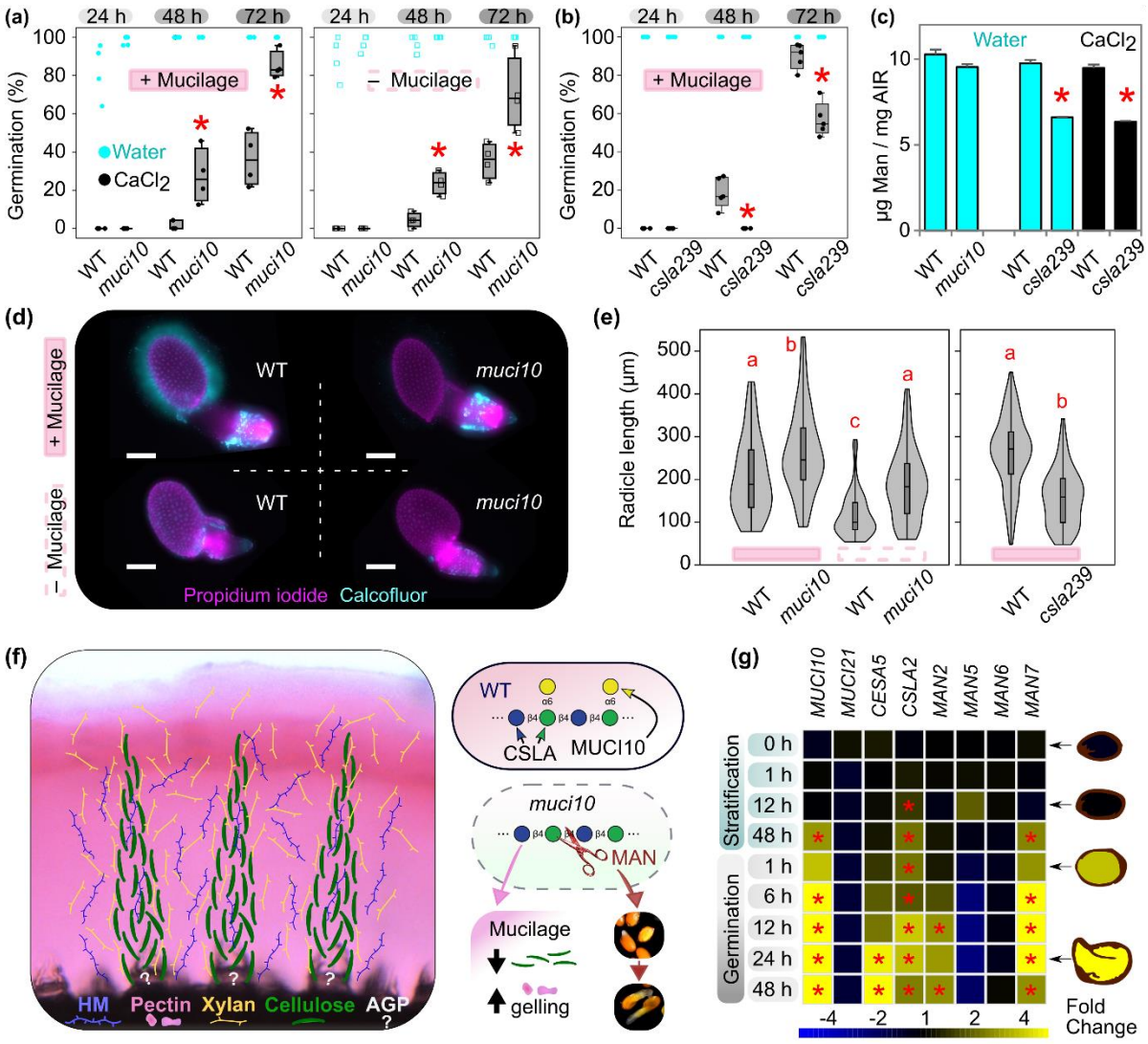

Fig. 4. Impact of mucilage and HM structure on germination.

(a) Germination of seeds with (+) or without (–; mill-extracted) mucilage. (b) Wild-type (WT) and *csla239* triple mutant. Box plots in (a) and (b) show four biological replicates. (c) Mannose content of germinated seeds. Data show the mean + SD of two technical replicates. (d) Dual cell wall staining and (e) radicle length of $CaCl_2$-treated seeds. Scale bars = 200 µm. Data in (c) to (e) corresponds to 72 h in (a) and (b) panels. (f) Model of wall polymers distribution in seed mucilage, and the effects of unbranched HM, which can be cleaved by β-1,4-mannanases (MAN). HM structure was drawn according to the Symbol Nomenclature for Glycans (SNFG). Xylan and HM have similar distributions but distinct roles. SOS5 maintains cellulosic rays but the exact location of this AGP remains unknown. (g) Transcriptional changes (asterisks; $P < 0.001$) during stratification and germination relative to dry seeds (0 h), profiled in GENEVESTIGATOR. Seed models are based on the eFP browser (http://bar.utoronto.ca).

bioRxiv preprint doi: https://doi.org/10.1101/2020.08.03.234708; this version posted August 4, 2020. The copyright holder for this preprint (which was not certified by peer review) is the author/funder, who has granted bioRxiv a license to display the preprint in perpetuity. It is made available under aCC-BY 4.0 International license.

References

Anderson CT, Carroll A, Akhmetova L, Somerville C. **2010**. Real-Time Imaging of Cellulose Reorientation during Cell Wall Expansion in Arabidopsis Roots. *Plant Physiology* **152**: 787–796.

Basu D, Tian L, Debrosse T, Poirier E, Emch K, Herock H, Travers A, Showalter AM. **2016**. Glycosylation of a Fasciclin-Like Arabinogalactan-Protein (SOS5) Mediates Root Growth and Seed Mucilage Adherence via a Cell Wall Receptor-Like Kinase (FEI1/FEI2) Pathway in Arabidopsis. *PLOS ONE* **11**: e0145092.

Ben-Tov D, Idan-Molakandov A, Hugger A, Ben-Shlush I, Günl M, Yang B, Usadel B, Harpaz-Saad S. **2018**. The role of COBRA-LIKE 2 function, as part of the complex network of interacting pathways regulating Arabidopsis seed mucilage polysaccharide matrix organization. *The Plant Journal* **94**: 497–512.

Berendzen K, Searle I, Ravenscroft D, Koncz C, Batschauer A, Coupland G, Somssich IE, Ülker B. **2005**. A rapid and versatile combined DNA/RNA extraction protocol and its application to the analysis of a novel DNA marker set polymorphic between Arabidopsis thaliana ecotypes Col-0 and Landsberg erecta. *Plant Methods* **1**: 4.

Goubet F, Barton CJ, Mortimer JC, Yu X, Zhang Z, Miles GP, Richens J, Liepman AH, Seffen K, Dupree P. **2009**. Cell wall glucomannan in Arabidopsis is synthesised by CSLA glycosyltransferases, and influences the progression of embryogenesis. *The Plant Journal* **60**: 527–538.

Goubet F, Misrahi A, Park SK, Zhang Z, Twell D, Dupree P. **2003**. AtCSLA7, a Cellulose Synthase-Like Putative Glycosyltransferase, Is Important for Pollen Tube Growth and Embryogenesis in Arabidopsis. *Plant Physiology* **131**: 547–557.

Griffiths JS, Crepeau M-J, Ralet M-C, Seifert GJ, North HM. **2016**. Dissecting Seed Mucilage Adherence Mediated by FEI2 and SOS5. *Frontiers in Plant Science* **7**: 1–13.

Griffiths JS, North HM. **2017**. Sticking to cellulose: exploiting Arabidopsis seed coat mucilage to understand cellulose biosynthesis and cell wall polysaccharide interactions. *New Phytologist* **214**: 959–966.

Griffiths JS, Šola K, Kushwaha R, Lam P, Tateno M, Young R, Voiniciuc C, Dean G, Mansfield SD, DeBolt S, *et al.* 2015. Unidirectional Movement of Cellulose Synthase Complexes in Arabidopsis Seed Coat Epidermal Cells Deposit Cellulose Involved in Mucilage Extrusion, Adherence, and Ray Formation. *Plant Physiology* **168**: 502–520.

Griffiths JS, Tsai AYL, Xue H, Voiniciuc C, Šola K, Seifert GJ, Mansfield SD, Haughn GW. **2014**. SALT-OVERLY SENSITIVE5 mediates arabidopsis seed coat mucilage adherence and organization through pectins. *Plant Physiology* **165**: 991–1004.

bioRxiv preprint doi: https://doi.org/10.1101/2020.08.03.234708; this version posted August 4, 2020. The copyright holder for this preprint (which was not certified by peer review) is the author/funder, who has granted bioRxiv a license to display the preprint in perpetuity. It is made available under aCC-BY 4.0 International license.

Hammer Ø, Harper DAT, Ryan PD. **2001**. PAST: Paleontological statistics software package for education and data analysis. *Palaeontologia Electronica* **4**.

Harpaz-Saad S, McFarlane HE, Xu S, Divi UK, Forward B, Western TL, Kieber JJ. **2011**. Cellulose synthesis via the FEI2 RLK/SOS5 pathway and CELLULOSE SYNTHASE 5 is required for the structure of seed coat mucilage in Arabidopsis. *The Plant Journal* **68**: 941–953.

He C, Yu Z, Teixeira Da Silva JA, Zhang J, Liu X, Wang X, Zhang X, Zeng S, Wu K, Tan J, *et al.* 2017. DoGMP1 from Dendrobium officinale contributes to mannose content of water-soluble polysaccharides and plays a role in salt stress response. *Scientific Reports* **7**: 1–13.

Iglesias-Fernández R, Rodríguez-Gacio MC, Barrero-Sicilia C, Carbonero P, Matilla A. **2011**. Three endo-β-mannanase genes expressed in the micropylar endosperm and in the radicle influence germination of Arabidopsis thaliana seeds. *Planta* **233**: 25–36.

Liepman AH, Wilkerson CG, Keegstra K. **2005**. Expression of cellulose synthase-like (Csl) genes in insect cells reveals that CslA family members encode mannan synthases. *Proceedings of the National Academy of Sciences of the United States of America* **102**: 2221–2226.

Mendu V, Griffiths JS, Persson S, Stork J, Downie AB, Voiniciuc C, Haughn GW, DeBolt S. **2011**. Subfunctionalization of Cellulose Synthases in Seed Coat Epidermal Cells Mediates Secondary Radial Wall Synthesis and Mucilage Attachment. *Plant Physiology* **157**: 441–453.

Narsai R, Law SR, Carrie C, Xu L, Whelan J. **2011**. In-Depth Temporal Transcriptome Profiling Reveals a Crucial Developmental Switch with Roles for RNA Processing and Organelle Metabolism That Are Essential for Germination in Arabidopsis. *Plant Physiology* **157**: 1342–1362.

North HM, Berger A, Saez-Aguayo S, Ralet M-C. **2014**. Understanding polysaccharide production and properties using seed coat mutants: future perspectives for the exploitation of natural variants. *Annals of Botany* **114**: 1251–1263.

Ralet M-C, Crépeau M-J, Vigouroux J, Tran J, Berger A, Sallé C, Granier F, Botran L, North HM. **2016**. Xylans Provide the Structural Driving Force for Mucilage Adhesion to the Arabidopsis Seed Coat. *Plant Physiology* **171**: 165–178.

Ruprecht C, Bartetzko MP, Senf D, Dallabernadina P, Boos I, Andersen MCF, Kotake T, Knox JP, Hahn MG, Clausen MH, *et al.* 2017. A synthetic glycan microarray enables epitope mapping of plant cell wall glycan-directed antibodies. *Plant Physiology* **175**: 1094–1104.

Saez-Aguayo S, Rondeau-Mouro C, Macquet A, Kronholm I, Ralet MC, Berger A, Sallé C, Poulain D, Granier F, Botran L, *et al.* 2014. Local Evolution of Seed Flotation in Arabidopsis. *PLoS Genetics* **10**: 13–15.

Schindelin J, Arganda-Carreras I, Frise E, Kaynig V, Longair M, Pietzsch T, Preibisch S,

bioRxiv preprint doi: https://doi.org/10.1101/2020.08.03.234708; this version posted August 4, 2020. The copyright holder for this preprint (which was not certified by peer review) is the author/funder, who has granted bioRxiv a license to display the preprint in perpetuity. It is made available under aCC-BY 4.0 International license.

Rueden C, Saalfeld S, Schmid B, *et al.* 2012. Fiji: an open-source platform for biological-image analysis. *Nature Methods* **9**: 676–682.

Schröder R, Atkinson RG, Redgwell RJ. **2009**. Re-interpreting the role of endo-β-mannanases as mannan endotransglycosylase/hydrolases in the plant cell wall. *Annals of Botany* **104**: 197–204.

Šola K, Dean GH, Haughn GW. **2019**. Arabidopsis Seed Mucilage: A Specialised Extracellular Matrix that Demonstrates the Structure–Function Versatility of Cell Wall Polysaccharides. *Annual Plant Reviews online* **2**: 1085–1116.

Sullivan S, Ralet M-C, Berger A, Diatloff E, Bischoff V, Gonneau M, Marion-Poll A, North HM. **2011**. CESA5 Is Required for the Synthesis of Cellulose with a Role in Structuring the Adherent Mucilage of Arabidopsis Seeds. *Plant Physiology* **156**: 1725–1739.

Voiniciuc C. **2016**. Quantification of the Mucilage Detachment from Arabidopsis Seeds. *BIO-PROTOCOL* **6**: 1–9.

Voiniciuc C. **2017**. Whole-seed Immunolabeling of Arabidopsis Mucilage Polysaccharides. *BIO-PROTOCOL* **7**: 1–10.

Voiniciuc C, Dama M, Gawenda N, Stritt F, Pauly M. **2019**. Mechanistic insights from plant heteromannan synthesis in yeast. *Proceedings of the National Academy of Sciences* **116**: 522–527.

Voiniciuc C, Günl M. **2016**. Analysis of Monosaccharides in Total Mucilage Extractable from Arabidopsis Seeds. *BIO-PROTOCOL* **6**: 1–12.

Voiniciuc C, Günl M, Schmidt MH-W, Usadel B. **2015a**. Highly Branched Xylan Made by IRREGULAR XYLEM14 and MUCILAGE-RELATED21 Links Mucilage to Arabidopsis Seeds. *Plant physiology* **169**: 2481–95.

Voiniciuc C, Schmidt MH-W, Berger A, Yang B, Ebert B, Scheller H V., North HM, Usadel B, Günl M. **2015b**. MUCILAGE-RELATED10 Produces Galactoglucomannan That Maintains Pectin and Cellulose Architecture in Arabidopsis Seed Mucilage. *Plant Physiology* **169**: 403–420.

Voiniciuc C, Yang B, Schmidt MH-W, Günl M, Usadel B. **2015c**. Starting to Gel: How Arabidopsis Seed Coat Epidermal Cells Produce Specialized Secondary Cell Walls. *International Journal of Molecular Sciences* **16**: 3452–3473.

Voiniciuc C, Zimmermann E, Schmidt MH-W, Günl M, Fu L, North HM, Usadel B. **2016**. Extensive Natural Variation in Arabidopsis Seed Mucilage Structure. *Frontiers in Plant Science* **7**: 1–14.

Western TL. **2012**. The sticky tale of seed coat mucilages: production, genetics, and role in

bioRxiv preprint doi: https://doi.org/10.1101/2020.08.03.234708; this version posted August 4, 2020. The copyright holder for this preprint (which was not certified by peer review) is the author/funder, who has granted bioRxiv a license to display the preprint in perpetuity. It is made available under aCC-BY 4.0 International license.

seed germination and dispersal. *Seed Science Research* **22**: 1–25.

Yang B, Voiniciuc C, Fu L, Dieluweit S, Klose H, Usadel B. **2019**. TRM4 is essential for cellulose deposition in Arabidopsis seed mucilage by maintaining cortical microtubule organization and interacting with CESA3. *New Phytologist* **221**: 881–895.

Yu L, Lyczakowski JJ, Pereira CS, Kotake T, Yu X, Li A, Mogelsvang S, Skaf MS, Dupree P. **2018**. The Patterned Structure of Galactoglucomannan Suggests It May Bind to Cellulose in Seed Mucilage. *Plant Physiology* **178**: 1011–1026.

Yu L, Shi D, Li J, Kong Y, Yu Y, Chai G, Hu R, Wang J, Hahn MG, Zhou G. **2014**. CELLULOSE SYNTHASE-LIKE A2, a glucomannan synthase, is involved in maintaining adherent mucilage structure in arabidopsis seed. *Plant Physiology* **164**: 1842–1856.

Zhong R, Cui D, Phillips DR, Ye Z-H. **2018**. A Novel Rice Xylosyltransferase Catalyzes the Addition of 2-O-Xylosyl Side Chains onto the Xylan Backbone. *Plant and Cell Physiology* **59**: 554–565.